Imaging endogenous gene expression: Ponomarev provides an overview and perspective on noninvasive genetic reporter imaging and previews an article on the development of a "universal approach" in this issue of *JNM*. . . . . ***Page 1035***

PET/CT monitoring in sarcomas: Benz and colleagues explore the extent of interobserver variability of standardized ^{18}F-FDG uptake parameters in assessing treatment response in patients with high-grade sarcomas. . . . . ***Page 1038***

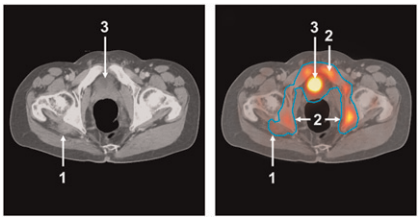

Dental implant artifacts in PET/CT: Nahmias and colleagues evaluate the efficacy of an algorithm that reduces metallic artifacts on CT images and the utility of this approach in quantification in PET images. . . . . ***Page 1047***

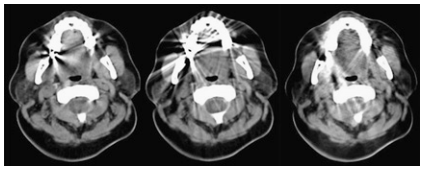

^{18}F-FDG uptake in lymph nodes: Nakagawa and colleagues investigate reactive lymph nodes in oral cancer to elucidate tracer-avid areas and discuss the potential of this information to correct for false-positive PET/CT findings in reactive lymphadenopathy during nodal staging. . . . . ***Page 1053***

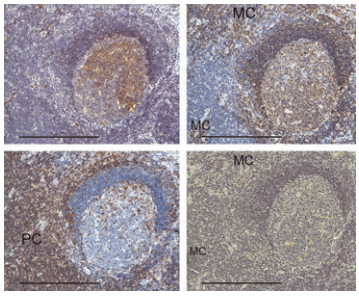

^{99m}Tc in somatostatin receptor imaging: Cwikla and colleagues compare tumor uptake and biodistribution of 2 novel tracers, ^{99m}Tc-TOC and ^{99m}Tc-TATE, in patients with gastrointestinal pancreatic neuroendocrine tumors. . . . . ***Page 1060***

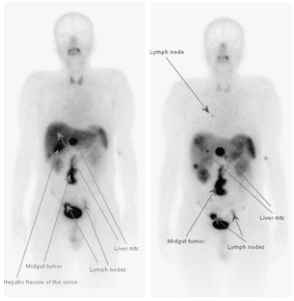

^{111}In-J591 for RIT: Pandit-Taskar and colleagues describe lesion detection, biodistribution, and dosimetry studies in humans using a monoclonal antibody targeting the prostate-specific membrane antigen and highlight the promise of this approach for radioimmunotherapy in prostate cancer. . . . . ***Page 1066***

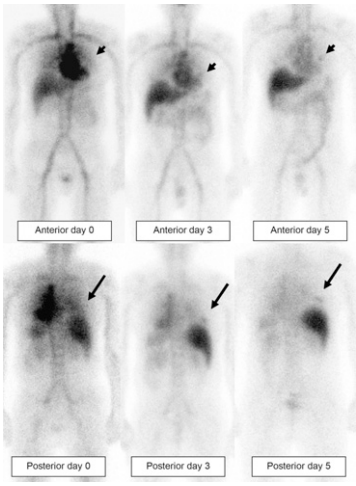

Motion-frozen gated SPECT: Suzuki and colleagues compare the diagnostic performance of standard SPECT with that of motion-frozen processing in myocardial perfusion scintigraphy detection of coronary artery disease in obese patients. . . . . ***Page 1075***

Multipinhole cardiac SPECT innovation: Steele and colleagues report on a triple-detector system configured to perform simultaneous stress and rest myocardial perfusion imaging using a protocol that permits direct diagnostic comparison with conventional rotational SPECT. . . . . ***Page 1080***

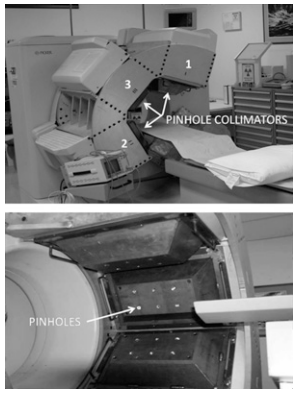

Coronary microvascular dysfunction: Sotgia and colleagues compare PET measurement of hyperemic myocardial blood flow with the extent of delayed contrast enhancement on MRI to explore the relationship between microvascular dysfunction and myocardial fibrosis in hypertrophic cardiomyopathy. . . . . ***Page 1090***

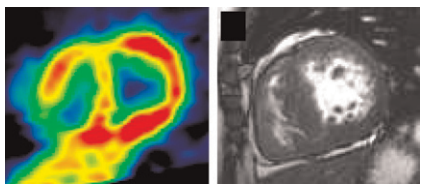

Automated PET partial-volume correction: Rousset and colleagues report on an atlas-based algorithm that automatically defines 3-dimensional regions of interest and apply this technique to partial-volume correction in dopamine receptor imaging in humans. . . . . ***Page 1097***

Improving PET in giant cell arteritis: Hautzel and colleagues introduce a receiver operating characteristic–based cutoff ratio to allow investigator- and experience-independent diagnosis of giant cell arteritis–related large-vessel inflammation with optimal sensitivity and specificity. . . . . ***Page 1107***

Instrumentation quality control: Zanzonico provides an educational overview of routine quality control procedures and guidelines for current nuclear medicine instrumentation. . . . . ***Page 1114***

Depth-of-interaction PET: Yang and colleagues describe the configuration of and initial results with a prototype small-animal scanner with depth-encoding detectors that facilitate simultaneous high sensitivity and high spatial resolution. . . . . ***Page 1132***

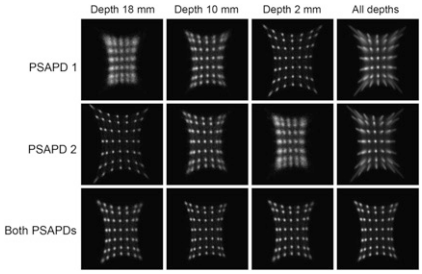

Electron-imaging ultrathin phosphor: Chen and colleagues report on the development of a sensitive, high-resolution system capable of direct imaging of radionuclide-produced β-particles, positrons, and conversion electrons in vivo. . . . ***Page 1141***

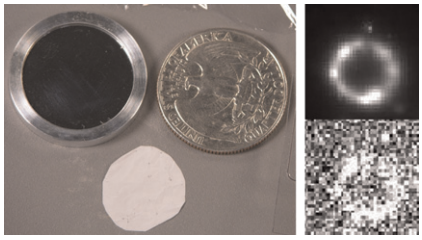

SMaRT imaging: Walls and colleagues introduce a generalizable strategy for imaging pre-mRNA levels in living subjects using spliceosome-mediated RNA *trans*-splicing, an approach that could provide the much-needed "universal" platform for probe design in molecular imaging of gene expression. . . . . ***Page 1146***

Radiosensitive intracerebral probe: Desbrée and colleagues describe the configuration and utility of a radiosensitive probe to measure PET radiotracer binding in vivo in mouse brain and discuss the potential of this approach for pharmacokinetic studies. . . . . ***Page 1155***

PET/bioluminescence T-cell imaging: Dobrenkov and colleagues report on an imaging methodology for in vivo assessment of biodistribution of adoptively transferred genetically modified human T-cells for treatment monitoring and prediction of tumor response in a systemic prostate cancer model. . . . ***Page 1162***

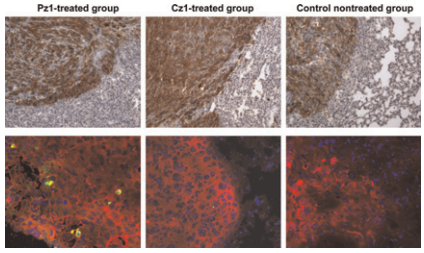

β-cell mass imaging: Kung and colleagues explore the potential utility of a novel vesicular monoamine transporter 2 imaging agent, FP-(+)-DTBZ, as a PET tracer for in vivo estimation of β-cell mass in the pancreas. . . . . ***Page 1171***

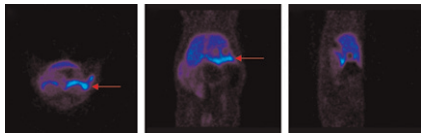

^{64}Cu-ATSM PET: Lewis and colleagues report on preclinical data on the effectiveness of this hypoxia-targeting radiopharmaceutical and on a crossover comparison of PET image quality and tumor uptake with ^{60}Cu-ATSM and ^{64}Cu-ATSM in cancer of the uterine cervix. . ***Page 1177***

Novel adenosine A_1/A_{2A} antagonist: Mihara and colleagues use PET to measure receptor occupancy of a novel radiotracer in monkeys to determine the degree of occupancy necessary to inhibit haloperidol-induced catalepsy. . . . . ***Page 1183***

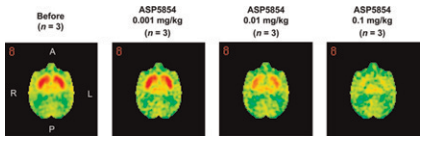

PET cardiac sympathetic neuronal imaging: Tipre and colleagues characterize the rat sympathetic nervous system using 3 radiotracers reflecting different subcellular mechanisms and discuss the translational potential of these techniques. . . . . ***Page 1189***

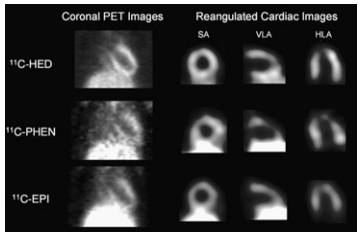

Risk prediction in hydronephrosis: Schlotmann and colleagues evaluate the functional and histomorphologic significance of delayed tissue transit of ^{99m}Tc-mercaptoacetyltriglycine in hydronephrosis. . . ***Page 1196***

Spheroid growth and PET tracers: Bergstrom and colleagues propose a translational imaging activity in which experiments in spheroids and xenografts are coupled to growth inhibition modeling and to related changes in tracer and biomarker kinetics. . . . ***Page 1204***

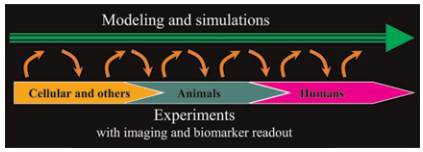

ON THE COVER

A 0.25-mm-diameter probe, simulated here, has been established as sufficiently sensitive for use in studies of PET tracer binding in the mouse brain. This probe, a new technical adaptation, will be invaluable for studies of serotonergic function in conventional or knock-out models of depression. The methodology can be used to address a wide range of issues relevant to the PET exploration of neurotransmitter systems in mouse models of neurologic or psychiatric diseases.

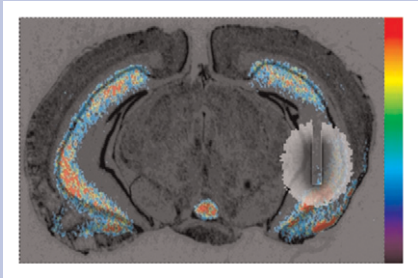

See page 1159.